Seismic assessment of a long-term lunar habitat

Carlos Patiño[a], Santiago Ruiz[a], Daniel Gomez[a,*], Alejandro Cruz[a], Shirley J. Dyke[b,c], Julio Ramirez[c]

[a]*School of Civil Engineering and Geomatics, Universidad del Valle, Cali, Valle del Cauca, Colombia.*
[b]*School of Mechanical Engineering, Purdue University, West Lafayette, IN, USA.*
[c]*Lyles School of Civil Engineering, Purdue University, West Lafayette, IN, USA*

Abstract

The establishment of secure earth-independent long-term lunar habitats has been envisioned by numerous government agencies and private companies. Recent advancements in assessing seismic hazards caused by shallow moonquakes have highlighted the importance of incorporating this phenomenon into the design of robust and resilient lunar structures. However, further research is required to explore lunar habitat design that considers seismic loads. This paper proposes assessing the structural response of a lunar habitat made of sulfur concrete covered with a regolith layer. The numerical model of the structure is subjected to gravitational, internal pressure and seismic loads. The seismic analysis of the structure is carried out using spectral and nonlinear time history methods. Conditional mean spectra for shallow moonquakes with return periods of 75, 475, 970 and 2475 years are used in the seismic analysis. The records used for the temporal analyses were ground motions that agree with a preliminary seismic hazard on the Moon. The results of temporal analyses reveal that shallow moonquakes with return periods greater than 475 years can lead to the loss of the global stability of the structure. Consequently, the findings imply that seismic loads have the potential to impose unacceptable demands on lunar structures constructed from in-situ materials like sulfur concrete. Hence, it is imperative to incorporate seismic considerations in the design process for developing resilient and long-term lunar habitats.

Keywords: Lunar habitat, Seismic analysis, Sulfur concrete, Shallow moonquake, Conditional mean spectrum, Lunar seismic hazard.

*Corresponding author.
Email address: daniel.gomez@correounivalle.edu.co (Daniel Gomez)

1. Introduction and general context

As humanity's interest in colonizing extraterrestrial bodies grows, engineers face the challenge of designing economical, reliable and safe extraterrestrial habitats. Among the celestial bodies considered for colonization, the Moon, being the closest to Earth, is the primary candidate [1–3]. The national space agencies of China, Russia, India, Canada, the United States and private companies are currently planning to establish a lasting human presence on the Moon [4]. An example of this is NASA's Moon to Mars Campaign, specifically through their Moon to Mars Objectives, which prioritize the development of habitation systems for crew members to live in deep space for extended periods of time [5]. A permanent lunar base would serve as an outpost for exploration, facilitate space tourism and in-situ resource utilization, enabling expeditions to other locations on the Moon's surface and beyond [6].

The design of future lunar bases must be adapted to the harsh environment and its associated withstand extreme conditions. Hazards such as high radiation levels, meteorite impacts, temperature variations and moonquakes pose a threat to lunar habitats [2, 7, 8]. Moonquakes, in particular, have been recorded and classified according to their depths and generation mechanisms [9, 10]. Shallow moonquakes with moment magnitudes M_w greater than 4.0 and lasting up to three hours have been identified as a significant hazard that must be considered in the design of long-term lunar habitats [11–14].

Ruiz et al. [13] conducted a probabilistic seismic hazard assessment (PSHA) at the Apollo 17 landing site and obtained hazard curves, uniform hazard spectra (UHS) and conditional mean spectra (CMS). UHS and CMS can be used to perform spectral and temporal seismic analyses. However, CMS provides a better representation of most moonquake response spectra that can occur at a given location [13, 15, 16]. The spectra obtained by Ruiz et al. [13] are initially preliminary and subject to modification when updated hazard models incorporate new information. Nevertheless, these spectra can still be used for purposes of seismic vulnerability assessment until further hazard studies are conducted.

Various studies have proposed different structural concepts for the design of long-term lunar habitats that can operate independently of Earth [2, 17, 18]. However, most studies have only considered loads generated by self-weight and internal pressure in their analysis [17, 19, 20]. A few studies have investigated the effect of meteorite impacts [21, 22] and thermal loads on structures [23–26]. Nevertheless,

research on evaluating the seismic behavior of lunar habitats has been limited [17]. Mottaghi and Benaroya [27] performed a seismic analysis of a magnesium structure with a sintered regolith foundation and sandbagged regolith cover using spectral methods and assuming elastic material behavior. More recently, Kalapodis et al. [28] assessed the seismic behavior of two-dimensional arches built with laser-sintered regolith using time history analysis. However, to the authors' knowledge, no studies have been conducted that perform nonlinear analysis of lunar habitats exposed to seismic demands derived from probabilistic seismic hazard assessment approaches.

This study aims to evaluate the seismic behavior of a lunar habitat made of regolith-based concrete and covered with regolith, using spectral and nonlinear time history analysis. A finite element model is developed to simulate the structure's response to gravitational, internal pressure and seismic loads. To perform the seismic analysis, the CMS obtained by Ruiz et al. [13] is employed. The stresses and strains generated in the structure by the different load cases are evaluated to assess its structural performance. This study provides valuable insight into the seismic response of lunar habitats when subjected to seismic loads, obtained from a probabilistic seismic hazard assessment approach.

2. Structural design of a long-term lunar habitat

The habitat's size and shape depend on the intended use and environmental conditions. A lunar habitat's design involves deciding on its geometry and the material used for construction. The choice of construction material should carefully consider factors such as availability, equipment requirements, construction costs and constructability. A comprehensive assessment of these variables is essential to ensure the successful realization of a robust and sustainable lunar habitat. Regolith is a readily available material with no transportation cost that may be used to build structures with 3D printing technology [18]. Additionally, regolith has the potential to yield materials with exceptional mechanical properties, serving as a natural protective shield against meteorite impacts, radiation and extreme temperature gradients.

2.1. Geometry definition

A lunar habitat must be pressurized to simulate earth-like atmospheric conditions to sustain human life for extended periods [29, 30]. Structures such as aircraft and gas tanks are engineered to withstand internal pressure, with their rounded shape facilitating the even distribution of stresses across their walls [31, 32].

Many proposed structural designs for lunar habitats follow this concept and feature rounded shapes [22, 24, 33, 34].

Since the Moon lacks an atmosphere, structures on its surface must endure extreme temperature fluctuations, significant amounts of radiation, abrasive dust and meteorite impacts [21]. As a solution, several authors have proposed using a layer of regolith to cover and protect habitats from these hazards [21, 27, 35]. This study proposes a cylindrical structure with spherical caps covered by a regolith layer as a potential lunar habitat design (Fig. 1).

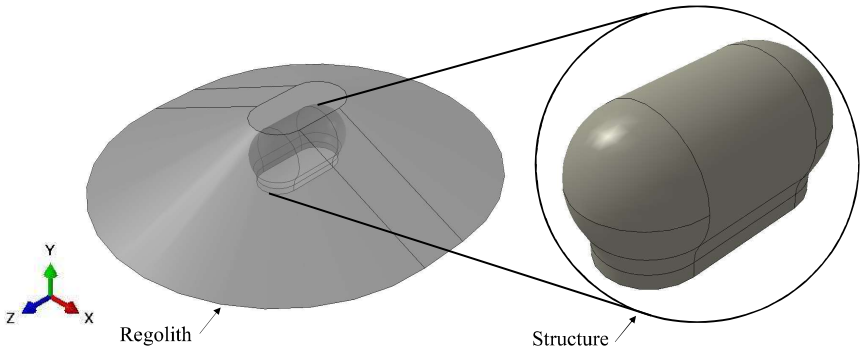

Fig. 1. Proposed lunar habitat under regolith layer.

The habitat volume plays a crucial role in establishing the maximum occupancy capacity for simultaneous inhabitants. The determination of both the habitat volume and the thickness of its cylinder walls constitutes integral aspects in the design process of the structure. Previous studies suggest that a design volume of 120 m^3 per person is suitable for long-term habitation in confined spaces [18, 29, 33]. In this study, we propose a structure designed to host ten astronauts, as shown in Fig. 2. The suggested dimensions of the structure are similar to those of other relevant studies and might be used as a two-story habitat [18, 33, 36, 37]. Since the structure is pressurized internally, it is possible to calculate the wall thickness as

$$t = \frac{p \times R \times SF}{\sigma_{tu}} \tag{1}$$

where p is the internal pressure, R is the radius of the cylinder, σ_{tu} is the tensile strength of the lunar concrete and SF is a design safety factor [38]. The design parameters used in the simulations are: p = 80 kPa, R = 5 m, σ_{tu} = 5.6 MPa [39] and SF = 5 [24]. Hence, a wall thickness of 0.35 m is proposed. The

wall thickness calculated using Eq. (1) might be decreased if additional metal or composite membranes are used to withstand the tensile stresses exerted by the internal pressure. Alternatives such as this should be evaluated in further research.

Protecting lunar structures from extreme temperature variations, meteorite impacts and radiation is critical to habitat design [18]. A regolith layer of 2.5 m and a structure's wall thickness of 0.35 m should keep radiation doses below the recommended limits [18, 40]. This regolith thickness protects the structure against meteorite impacts of up to 800 g [22]. In addition, the regolith layer provides thermal insulation to the structure by minimizing temperature fluctuations within the soil layer to ± 2.8°C [41]. The determination of the slope of the regolith shield is based on the internal friction angle of the lunar soil, which is equal to 40° [42]. A slope angle of 25° is proposed, which corresponds to a safety factor of 1.8 [43]. The dimensions of the regolith shield are shown in Fig. 2(c and d).

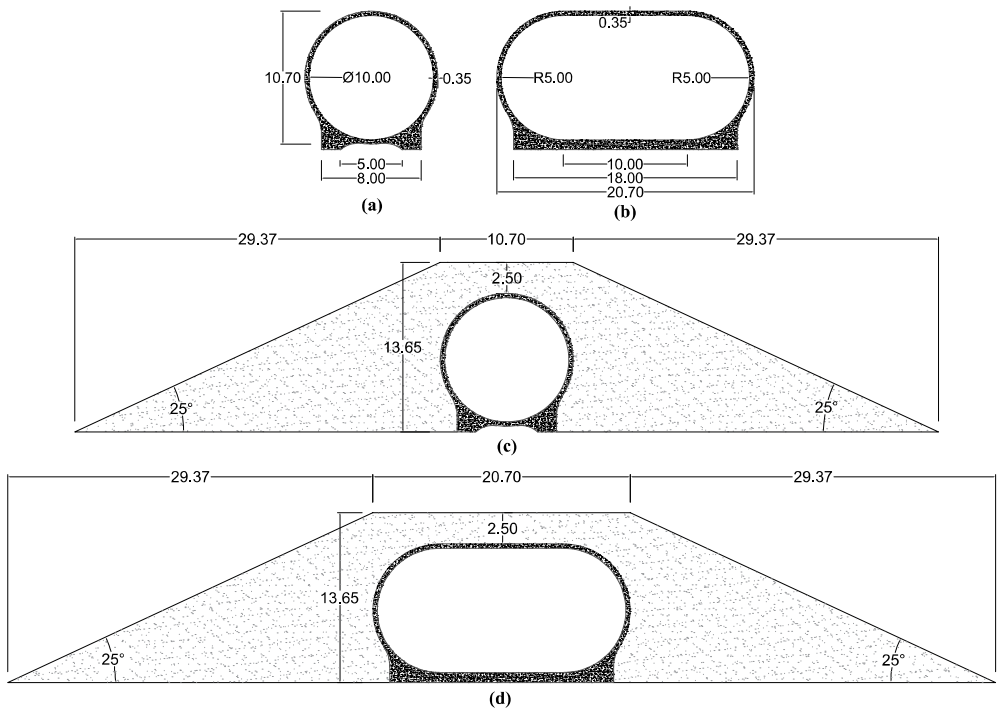

Fig. 2. Lunar structure plans. (a) Transversal and (b) longitudinal cross-section of the structure without regolith layer. (c) Transversal and (d) longitudinal cross-section including the regolith layer. The dimensions in the figure are given in meters.

Although the proposed soil thickness provides adequate protection against meteorite impacts, radiation and extreme temperature variations, it involves significant material movement and may be susceptible to displacement due to external factors [44]. Reshaping the soil to its initial geometry may be time-consuming and resource-intensive. Therefore, it would be worthwhile to assess protection alternatives, such as incorporating additional polyethylene layers to reduce the volume of soil required for the structure.

2.2. Construction material

The construction of lunar habitats can be achieved by using transported materials or in-situ resources [2]. However, transporting construction materials from Earth is deemed infeasible due to high costs and limited spacecraft cargo capacity [24, 28, 45, 46]. Therefore, employing lunar resources for manufacturing materials is an attractive option for constructing lunar settlements. Lunar regolith, a soil layer formed by regular meteorite impacts on the lunar surface, is one of the most abundant materials on the Moon [47]. Numerous authors have suggested using lunar regolith for producing construction materials for lunar bases [22, 48, 49].

Regolith samples collected during the Apollo 11 and 17 missions indicated high sulfur content of up to 2000 ppm [47]. Melting sulfur in regolith and combining it with fine and coarse regolith has been demonstrated in experiments to produce lunar sulfuric concrete [39, 40, 50]. While continuous research efforts are being made to enhance its performance in vacuum and low-gravity conditions, sulfur concrete remains an attractive option for the development of lunar structures owing to its availability, notable strength and enduring properties [40, 50–52]. The use of this material has been explored in the construction of some elements, such as bricks and plates, for extraterrestrial structures [53, 54]. Although some researchers [55, 56] have shown that glass fibers might be obtained from regolith for use as reinforcement in lunar sulfuric concrete, this study proposes using unreinforced sulfur concrete as the primary building material for the lunar habitat structure. Our research suggests using concrete made entirely of in-situ material and therefore has no transported reinforcement. As a result, the material is in charge of resisting compressive and tensile stresses. Table 1 summarizes the current understanding of the mechanical properties of the regolith and sulfur concrete. It is important to note that the lunar sulfur concrete has not been tested at scale for structural applications. Therefore, its mechanical properties may vary considerably when this material is used in large-scale structures. The manufacturing process, composition and curing process might generate high variations in the material's mechanical properties. Hence, future research may perform a parametric study to evaluate the variations

in the structural response as a function of changes in the mechanical property values. Thus, the proposed structure is notional and the material properties at scale are assumed for purposes of this analysis.

Table 1. Mechanical properties of regolith and lunar sulfur concrete.

Parameter	Regolith	Reference	Sulfur concrete	Reference
Density (kg·m^{-3})	1500	[57]	2330	[58]
Angle of repose (°)	40	[42]	-	-
Young modulus (MPa)	4.6	[59]	20700	[39]
Poisson ratio	0.17	[60]	0.31	[61]
Compressive strength (MPa)	-	-	31	[40]
Mean tensile strength (MPa)	-	-	5.6	[39]

While the elastic mechanical properties presented in Table 1 are suitable for conducting a spectral analysis of the lunar habitat, additional information on the elastoplastic behavior of lunar sulfuric concrete is needed to perform a nonlinear seismic analysis. However, research on the plastic phase behavior of this material is currently lacking. To approximate its nonlinear behavior under compression, the Eurocode provides a suitable definition [62], as

$$\sigma_c = \sigma_{cu} \frac{k\eta - \eta^2}{1 + (k-2)\eta} \tag{2}$$

with

$$\eta = \frac{\epsilon_c}{\epsilon_{cu}} \tag{3}$$

$$k = \frac{1.05 E \epsilon_{cu}}{\sigma_{cu}} \tag{4}$$

where σ_c is the compression stress, σ_{cu} is the maximum compression stress, ϵ_c is the compression strain, ϵ_{cu} is the strain at the peak compression stress and E is Young's modulus. In this study a typical value for plain concrete of $\epsilon_{cu} = 2{\times}10^{-3}$ is used [63], the values for E and σ_{cu} are taken from Table 1.

The assumed linear elastoplastic nature of lunar sulfur concrete in tension can be accounted for as follows. Micro-cracks appear in the material leading to plastification at around 50% to 85% of its maximum tensile strength σ_{tu} [64, 65]. This study assumes that the material reaches $0.5\sigma_{tu}$ when the initial micro-cracks

appear, producing plastification i.e. the material remains elastic until it reaches a total tensile strain $\epsilon_t = 1.35\times10^{-4}$ or is subjected to a tensile stress $\sigma_t = 2.8$ MPa. At this point, the appearance of micro-cracks leads to a degradation in the stiffness of the lunar sulfuric concrete. As no data on the material's stiffness in the plastic range is available, it is assumed that the material's stiffness in this range is 90% of the elastic stiffness. Therefore, when $\sigma_t = \sigma_{tu}$, the total and plastic strain are $\epsilon_t = 2.85\times10^{-4}$ and $\epsilon_p = 1.5\times10^{-5}$, respectively. Once the concrete reaches its maximum tensile strength, macro-cracking occurs and there is an immediate loss of strength. The stress-strain curve of the lunar sulfuric concrete used in this study is shown in Fig. 3. It is important to note that the mechanical behavior of lunar sulfur concrete may differ significantly from that of plain concrete due to its unique properties, and further research is required to fully understand its behavior under lunar conditions.

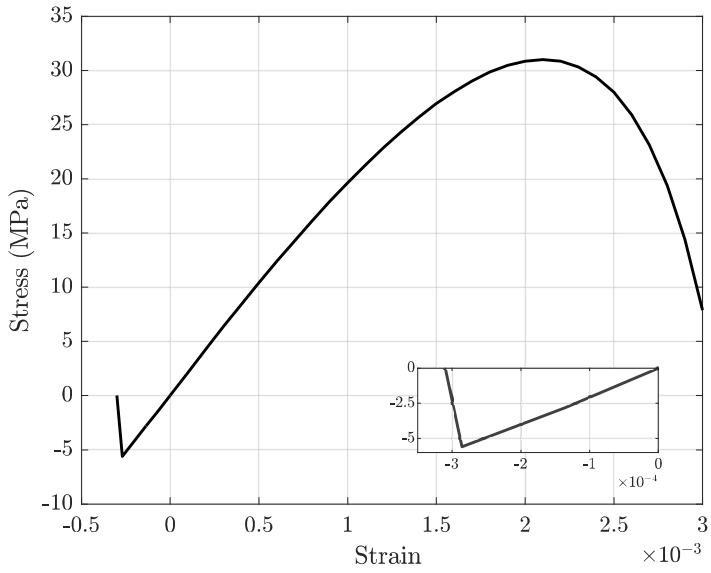

Fig. 3. Constitutive curve for lunar sulfur concrete.

2.3. Lifetime of the structure

Defining the expected lifespan of a structure is an important factor in its design. The structure's lifespan is affected, among other factors, by extreme temperature gradients and permanent radiation [66]. The aging in the structures is caused by changes and degradation of the mechanical properties of its materials. This issue is

caused by material fatigue from repetitive cycles of expansion and contraction [67, 68] and intense exposure to ionizing radiation [1, 2, 69]. However, due to the focus and scope of this study, we will not consider the potential impact of the structure's interaction with these environmental agents on its lifetime. Lunar structures are expected to have a comparable lifespan to their terrestrial counterparts, typically ranging from 30 to 100 years, due to their high initial costs [70]. Therefore, this study considers a lunar structure with an anticipated lifespan of 50 years.

3. Methods

3.1. Numerical modelling

A 3D numerical model is developed using the Abaqus software [71] to conduct numerical analyses of the lunar structure and regolith layer (Fig. 4). To discretize the continuous problem domain, a mesh of tetrahedral elements with ten nodes each is chosen for their ability to accommodate curved and complex geometries. This element type was also chosen for its ability to represent the structure's dynamic characteristics and to enable automatic meshing of the model geometry. To ensure the accuracy and efficiency of the simulation, a convergence analysis to determine the appropriate mesh size is performed. We found that a mesh comprising 12274 elements for the structure and 28528 for the regolith layer provided mesh-independent results.

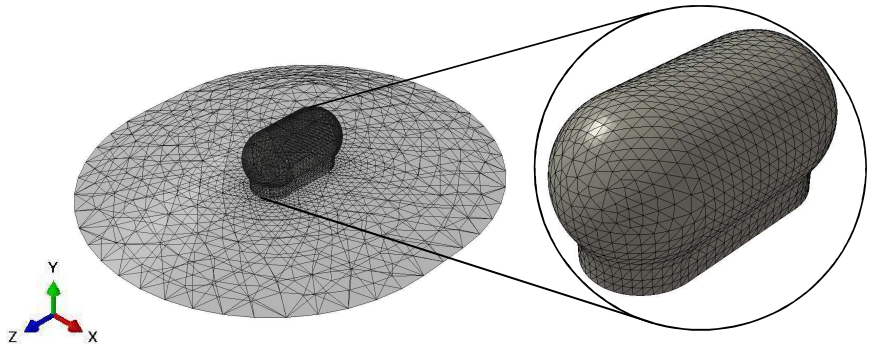

Fig. 4. Finite element model of the structure under regolith layer. The mesh of the structure and the regolith shield are composed of 12274 and 28528 tetrahedral second-order elements, respectively.

This study assumes that the regolith and the structure will be simply supported on bedrock. Therefore, translational constraints are applied to the structure's base and the regolith layer's lower part as boundary conditions. The interface's tangential and normal properties are defined to simulate the contact between the concrete

and regolith layers. The tangential behavior is modeled using a friction coefficient (μ) of 0.3, which is a typical value for the interaction between concrete and soil. In this study, it is assumed that the friction between the soil and the structure follows the Coulomb friction model. A hard contact condition is employed for the normal behavior of the contact. The model considers that the regolith acts in the linear elastic regime, while the sulfuric concrete has an elastoplastic behavior as described above.

The model is subjected to three specific load cases to account for the different loading conditions the structure may experience during its operational life. These load cases represent the initial state of the structure (self-weight only), the pressurized state (self-weight and internal pressure) and the normal operating conditions subjected to seismic excitation (self-weight, internal pressure and seismic loading). Dynamic modal spectral analysis and nonlinear time history analyses are performed to examine the seismic behavior of the structure.

3.2. Gravitational and internal pressure loads definition

Before conducting the seismic analysis, the structural model needs to be preloaded with the gravity load and internal pressure. To consider the effects of gravity, the model is subjected to lunar acceleration, which is equivalent to one-sixth of earth's gravity, corresponding to 1.62 $m \cdot s^{-2}$ [2]. Additionally, the structure is pressurized to reach pressure levels similar to those experienced on Earth's surface, typically ranging from 70 to 100 kPa [41, 72]. In this study, an internal pressure of 80 kPa is applied to the structure, under this level of pressure the structures can support life [72].

3.3. Seismic analysis

The Apollo Seismic Network (ASN) detected, digitized and transmitted approximately 13000 seismic events on the Moon, which were then recorded by one of the Deep Space Network ground stations on earth [73]. The ASN was composed of long and short-period sensors with sampling rates of 7 Hz and 53 Hz, respectively. The long-period sensors could capture both vertical and horizontal motions, while the short-period sensors were sensitive only to vertical motions [74]. It should be noted that due to the low sampling rate of the long-period sensors, the seismic information captured is very limited. The seismic stations recorded diverse seismic vibrations originating from various sources, encompassing both internal lunar events and external environmental phenomena [9, 75]. By analyzing the seismograms, different seismic signals were classified based on characteristics such as hypocentral location, generation mechanism and magnitude, among others

[76]. Based on this analysis, researchers have categorized lunar seismic activity into five types of moonquakes: deep, thermal, shallow, meteorite impacts and unclassified events [10, 77–79].

The most energetic and rare type of event detected on the Moon are shallow moonquakes, also referred to as High-frequency Teleseisms (HFT) [27, 76]. During the Passive Seismic Experiment (PSE) a total of 28 HFT events with focal depths between 50 and 200 km were detected [76, 80]. The recorded shallow moonquakes have been determined to reach M_w up to 4.1 [11–13, 81]. Although the ASN recorded few events during its operation, geological evidence indicates that shallow moonquakes are relatively frequent events on the Moon [82]. The generation mechanisms of these events are unknown; however, recent findings by Watters et al. [83] suggest that they are associated with young thrust fault scarps. According to its magnitude, shallow moonquakes can be as strong as intermediate magnitude earthquakes or the strongest marsquakes recorded by the InSight [13, 84]. Typical shallow moonquakes last several hours, which is much longer than terrestrial or Martian quakes [27, 84]. These characteristics make this hazard capable of inflicting significant damage to future long-term lunar bases. Consequently, it is necessary to incorporate these factors into the design considerations of such structures [12, 13, 85]. Despite the limitations on our understanding of lunar seismology, we aim to realistically assess the seismic risk of a structure on the lunar surface by using the limited available information.

3.3.1. Site selection

The structure's location must be determined to define the hazard generated by shallow moonquakes. The South Pole of the Moon offers several advantages for establishing a sustainable long-term human base on the lunar surface, leading numerous researchers to propose it as the site for the first lunar habitats [86–88]. However, despite its potential, there is currently no probabilistic seismic hazard study specifically conducted for this location [85], resulting in a lack of available seismic spectra for designing future bases in this area. In contrast, Ruiz et al. [13] conducted a seismic hazard assessment for the Taurus-Littrow Valley, the landing site of the Apollo 17 mission (20.19° N and 30.76° E). The primary seismic activity in this region is associated with the Lee Lincoln lobate scarp, a fault that spans approximately 14 km and has been identified as seismically active [83]. Based on the estimates provided by Ruiz et al. [13], the Lee-Lincoln fault is capable of generating shallow moonquakes with a magnitude of 6.4 M_w. These findings are utilized in this study to select the Apollo 17 Moon landing site as the designated location for the lunar habitat.

3.3.2. Modal spectral analysis

The dynamic characteristics of the structure and the spectra that will be used as seismic demand are necessary features to perform a dynamic modal spectral analysis (DMSA) of the structure. The modes and frequencies of vibration represent the dynamic properties of the structure, while the spectra are obtained from the hazard analysis conducted at the specific site where the structure will be located. This information enables the assessment of the structure's response for each vibration mode, which can then be combined to obtain the overall structural response.

The study utilizes the Lanczos algorithm available in the Abaqus libraries [71, 89], to calculate the model's natural frequencies and mode shapes of vibration. Fig. 5 displays the first six vibration modes with associated frequencies ranging from 1.20 Hz to 1.49 Hz. Although the modal analysis considers the structure with regolith, this layer is excluded from the graphical representation in Fig. 5 to provide a more precise visualization of the mode shapes of the structure. The spectral modal dynamic analysis focuses on the first six vibration modes, as they contribute to over 90% of the mass participation in the seismic response of the structure. In traditional structural design, this modal truncation is allowed because the residual modal mass of the high-order modes is small compared to the total mass of the structure. Although our analysis only considers the modes mentioned above, the mesh is able to capture high-frequency modes.

The first PSHA on the Moon was performed by Ruiz et al. [13]. PSHA techniques were used to obtain hazard curves, hazard deaggregation, UHS and CMS for the Apollo 17 landing site. Although both UHS and CMS may be used for structural seismic analysis, CMS provides a better representation of most response spectra of quakes at a location. Therefore, CMS is used in the seismic analysis of the proposed lunar habitat [13, 15, 16]. To assess the structure's response due to moonquakes with different intensities, this study generates four CMS for shallow moonquakes with return periods (T_r) of 75, 475, 970 and 2475 years (exceedance probabilities of 50%, 10%, 5% and 2% in 50 years, respectively), corresponding to frequent, rare, very rare and extremely rare quakes [90]. The CMS for the fundamental vibration period of the structure T^* = 0.83 s and different return periods generated for this study are shown in Fig. 6. These spectra are used as seismic demand in the DMSA of the structure.

The complete quadratic combination (CQC) method is employed in this paper to combine the responses and determine the total structural response to seismic loads. The multiple direction square root of the sum of squares (SRSS) method is utilized to implement the directional combination of the seismic demand.

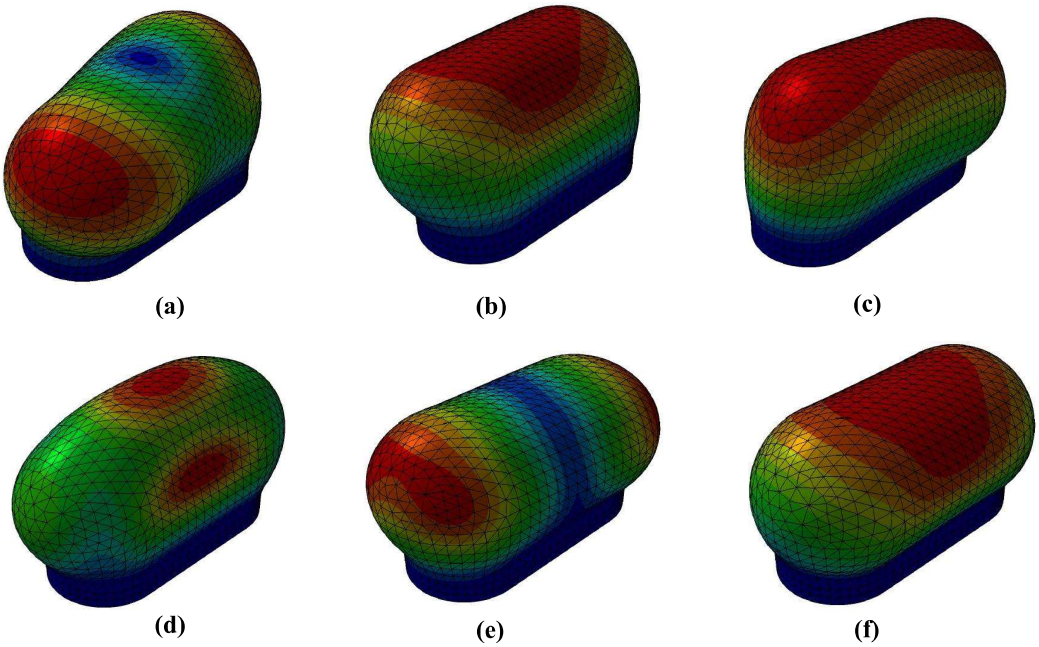

Fig. 5. Mode shapes of vibration with related frequencies of (a) 1.20 Hz, (b) 1.24 Hz, (c) 1.26 Hz, (d) 1.39 Hz, (e) 1.40 Hz and (f) 1.49 Hz.

3.3.3. Nonlinear response history analysis

In nonlinear response history seismic analysis (NRHA), ground motions (GM) representing the seismic demand are applied to the structure. This section synthesizes the literature on GM selection methods and delineates the outcomes derived from a nonlinear response analysis conducted on the proposed lunar habitat. The GM may be historical seismic records of events representative of the hazard at the study site with similar generation mechanisms, magnitudes and distances [91]. However, if such records are unavailable, artificial seismograms or modified records that match the seismic hazard at the study site are often used [92]. In this study, the seismic analysis utilizes the modification of existing GM. Specifically, seven pairs of horizontal acceleration records from the 28 shallow moonquakes recorded by the ASN are arbitrarily selected and modified. Record modification is a widely used method for obtaining hazard-compatible seismic signals for temporal seismic analysis [93, 94]. Table 2 presents the modified GM along with their corresponding date of occurrence, recording station, peak ground acceleration (PGA) and distance to the seismic stations. The response spectra of these modified GM are calculated and shown in Fig. 7.

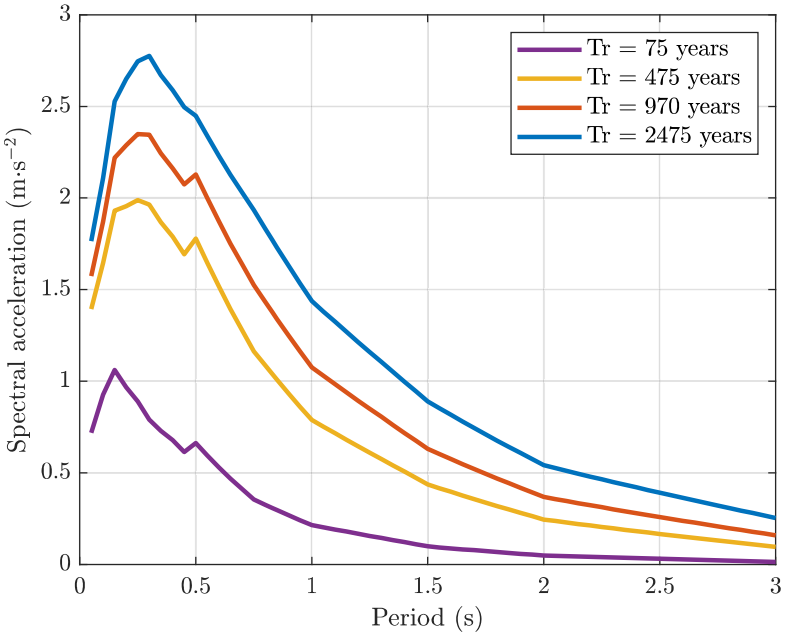

Fig. 6. Conditional mean spectra for shallow moonquakes with T_r of 75, 475, 970 and 2475 years.

Table 2. Selected unscaled GM to be used in NRHA. Distance to stations taken from [11].

GM	Date	Station (component)	PGA (m·s^{-2})×10^{-8}	Distance (km)
1	1971/04/17	12 (x)	3.52	
2	1971/04/17	12 (y)	2.80	
3	1971/04/17	14 (x)	7.51	1970
4	1971/04/17	14 (y)	9.50	
5	1973/03/13	12 (x)	5.28	
6	1973/03/13	12 (y)	6.87	
7	1973/03/13	16 (x)	14.94	2380
8	1973/03/13	16 (y)	17.69	
9	1975/01/03	14 (x)	12.5	2320
10	1975/01/03	14 (y)	12.0	
11	1975/01/03	16 (x)	23.4	2930
12	1975/01/03	16 (y)	39.6	
13	1976/03/06	14 (x)	3.95	490
14	1976/03/06	14 (y)	7.10	

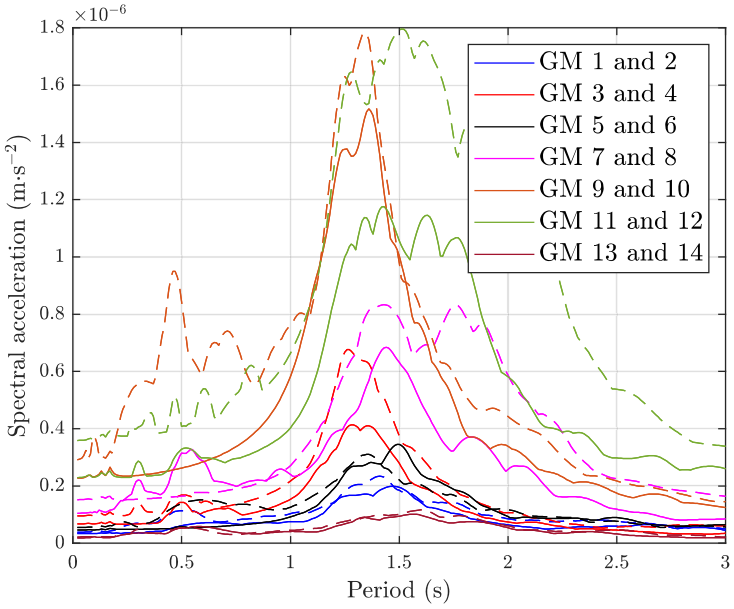

Fig. 7. Five percent damped elastic response spectra of the unscaled records (x-component in continuous and y-component in dashed line) of the seven selected shallow moonquakes.

The PGA and spectral acceleration (SA) of the analyzed ground motions are found to be significantly low, mainly due to the long distance between the epicenters and the seismic stations where these events were recorded. However, previous studies by Ruiz et al. [13], Mohanty et al. [82] and Mishra and Kumar [85] have demonstrated that the seismic hazard is considerably high at the study site and other locations on the Moon. Therefore, the original seismograms used for temporal analyses have been scaled to represent the hazard levels determined in the study by Ruiz et al. [13]. In this study, the scaling process involves iteratively modifying the original signal's Fourier spectrum until the modified moonquakes' response spectrum matches the target spectrum, as determined in Section 3.3.2. This procedure is valid regardless of the model's nonlinearity because it affects only the input signals. This iterative process, similar to that performed by Ferreira et al. [92], ensures that the modified GM exhibits a shallow moonquake's time and frequency characteristics from the analyzed seismogenic source. Fig. 8 illustrates an example of the outcome achieved through the modification process of a GM to ensure its compatibility with a shallow moonquake event with T_r of a 475-year return period. The CMS and scaled response spectra for different seismic intensity levels are depicted in Fig. 9. The adjustment interval of the spectra ranges from $0.2T^*$ to $1.5T^*$, covering the period range where the structural response of the

lunar habitat is most sensitive. The iterative process is continued until the spectral ordinates of the response spectrum within the interval of interest reach at least 90% of the target spectrum. A similar fitting criterion is also required in the NRHA of highly complex terrestrial structures, such as nuclear power plants [95].

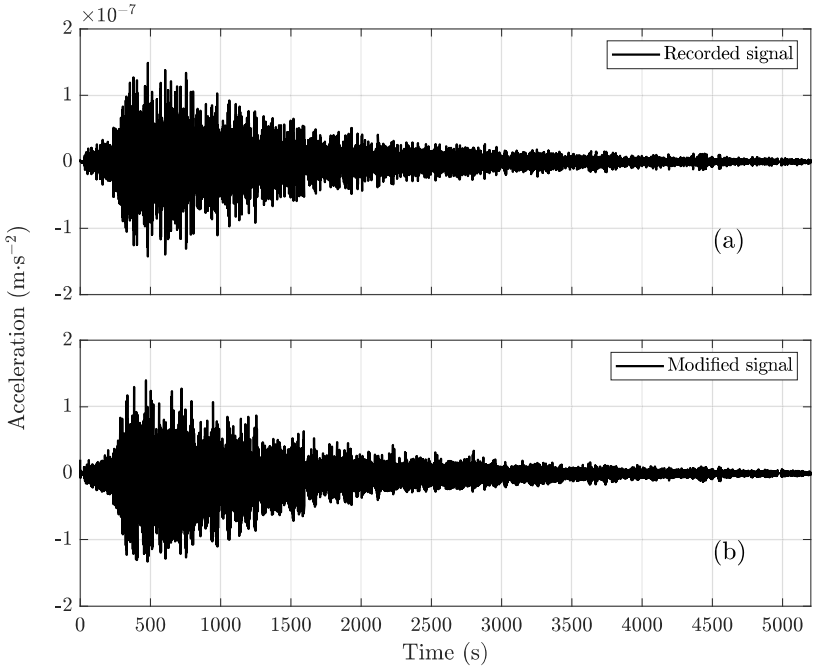

Fig. 8. Sieismograms (a) recorded and (b) modified of the x-component of the shallow moonquake event registered on 1975/01/03 by the Apollo 14 station.

The NRHA method enables the assessment of the plastic behavior of materials, the degradation of material strength and the identification of damage locations within a structure. This study utilizes a constitutive model for concrete that incorporates plastic behavior and degradation of mechanical properties. The proposed model, initially introduced by Lubliner et al. [96], subsequently modified by Lee and Fenves [97], has been adapted for implementation in Abaqus [71]. The concrete damage plasticity model (CDPM) effectively accounts for irreversible damage resulting from various failure mechanisms in concrete structures with low confinement levels [71]. The CDPM comprises a stress-strain relationship, a stiffness degradation law, a yield condition and a flow rule [97]. The following equation defines the stress-strain relationship within the CDPM:

$$\sigma = (1-d)D_0^{el} : (\epsilon - \epsilon^{pl}) = D^{el} : (\epsilon - \epsilon^{pl}) = D^{el} : \epsilon^{el} \tag{5}$$

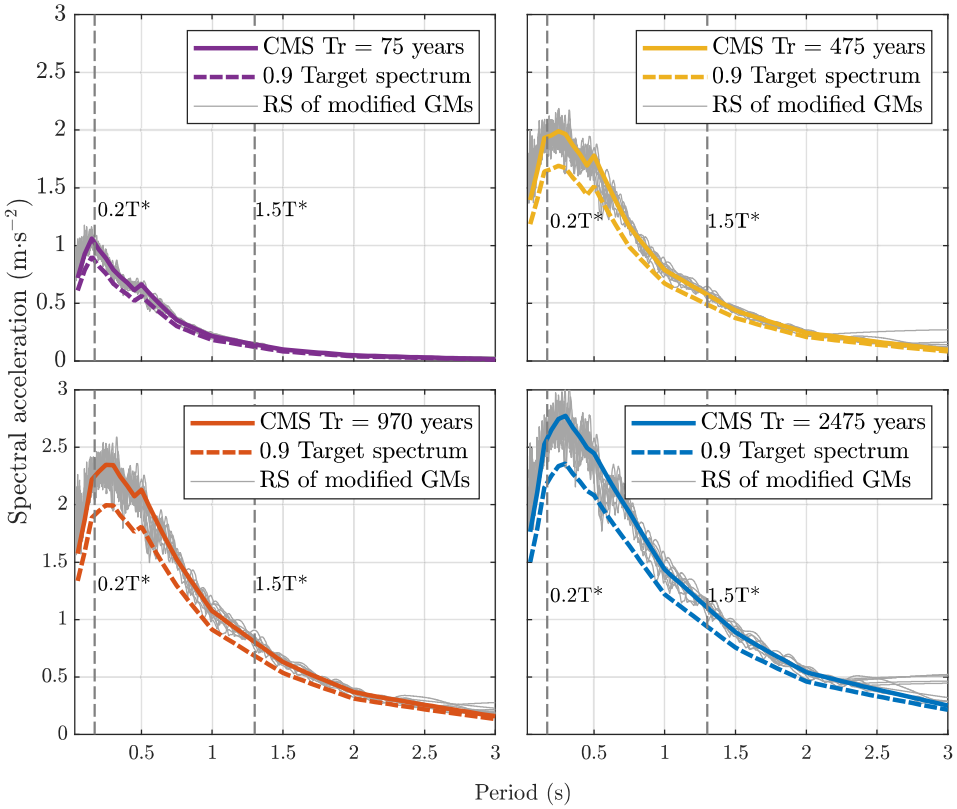

Fig. 9. Scaled Response Spectra (RS) and CMS of T_r of 75, 475, 970 and 2475 years.

where σ is the Cauchy stress tensor, $\epsilon = \epsilon^{el} + \epsilon^{pl}$ is the deformation tensor, ϵ^{el} is the elastic part of the deformation tensor, ϵ^{pl} is the plastic part of the deformation tensor, D_0^{el} is the elastic stiffness of the material (before damage), $D^{el} = (1 - d)D_0^{el}$ is the degraded elastic stiffness and d is an elastic stiffness degradation parameter [71]. The CDPM assumes that the stiffness degradation is isotropic, thus, it is characterized only through the damage variable d. We assume that the damage in lunar sulfuric concrete, a granular constituted solid, is stochastically isotropic. The effective stress tensor is defined by

$$\overline{\sigma} = D_0^{el} : (\epsilon - \epsilon^{pl}). \tag{6}$$

The effective stress tensor is related to the damage variable by the following expression:

$$d = d(\overline{\sigma}, \tilde{\epsilon}^{pl}) = 1 - \frac{\sigma}{\overline{\sigma}} \tag{7}$$

where $\tilde{\epsilon}^{pl}(\tilde{\epsilon_c}^{pl}, \tilde{\epsilon_t}^{pl})$ represents the hardening and softening variables for compression $\tilde{\epsilon_c}^{pl}$ and tension $\tilde{\epsilon_t}^{pl}$, respectively.

In this study, typical values reported in the literature are employed to model the plastic behavior of concrete. The dilation angle, eccentricity and viscosity parameters are set to 35°, 0.1 and 0.0005, respectively, as reported by [98]. The parameter K_c has an assigned value of 2/3 and the ratio of f_{b0}/f_{c0} is set to 1.16, as reported by Xiao et al. [99]. These values are typically used for concrete [98–101]. These parameter values are incorporated into the CDPM to accurately capture the effects of irreversible damage on the mechanical properties of concrete.

4. Results and discussion

4.1. Initial structural analysis of the habitat subjected to static loads

This study examines two load cases to assess the behavior of the proposed habitat under sustained loads. The first load case considers the gravitational effect from the structure's self-weight and the regolith layer, while the second load case adds an internal pressure of 80 kPa on the internal walls.

The first load case represents the initial conditions after construction. Tensile stresses are examined in Fig. 10 (a) and (b), where it is observed that the maximum tensile stress (σ_t) occurs at the connection between the main structure and its supports, reaching 1.0 MPa, which corresponds to approximately 17.68% of the maximum tensile stress of sulfur concrete (σ_{tu}). Stresses near $0.15\sigma_{tu}$ are observed on the outer surfaces of the cylindrical structure's lateral walls, indicating the habitat's ability to withstand lunar gravity effectively. These findings demonstrate the structural performance and integrity of the proposed habitat.

The second load case, which represents the serviceability conditions of the structure without lunar hazards, exhibits a different distribution of tensile stresses compared to the first load case. Tensile stresses are more uniformly distributed throughout the walls of the structure. Fig. 11 (a) and (b) illustrate the spatial distribution of tensile stresses outside and inside the structure, respectively. The load case reveals that the maximum tensile stress is localized on the interior side of the joint between the cylindrical portion of the main structure and the supports, reaching a magnitude of 2.22 MPa, equivalent to approximately $0.40\sigma_{tu}$. These findings suggest that internal pressure influences the structural design more than gravitational loads. The maximum stresses are concentrated in the junction

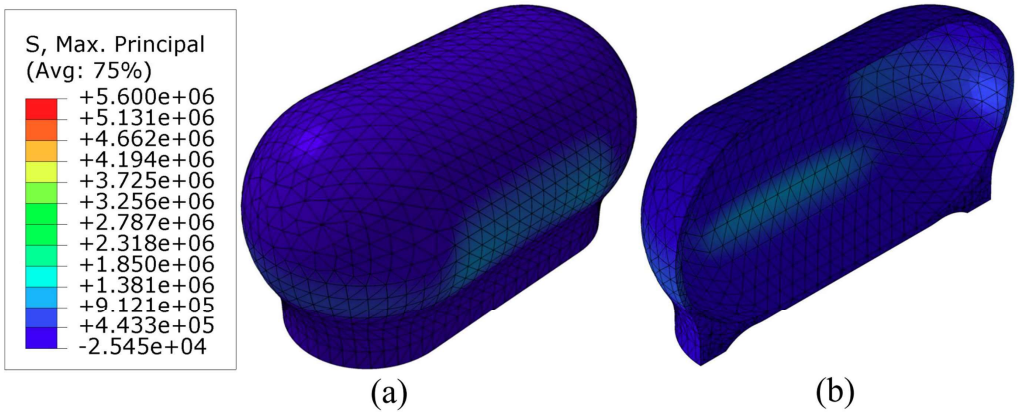

Fig. 10. Tensile stresses distribution generated by the gravitational load. (a) External view and (b) transversal cut view.

zones between the supports and the main cylindrical structure due to the abrupt change in geometry, leading to stress concentration zones. However, the structure's weight and the regolith layer mitigate the stresses induced by the internal pressure, reducing tensile stresses throughout the structure. Notably, the regolith layer is crucial in minimizing the adverse effects of radiation, meteorite impact and internal pressure on the structure's integrity. These results provide valuable insights for designing and evaluating the proposed habitat under normal operational conditions.

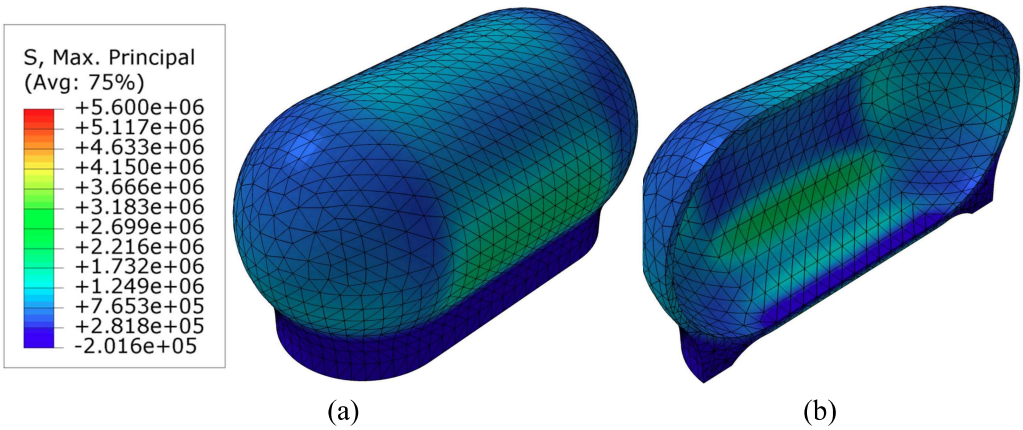

Fig. 11. Tensile stresses generated by internal pressure load. (a) External view and (b) transversal cut view.

4.2. Seismic analysis

The seismic response of the proposed lunar habitat is evaluated using the DMSA and NRHA methods. The spectral analysis provided a straightforward and efficient means of obtaining the structural response under seismic loads. Additionally, temporal analyses are performed to consider the influence of inertial forces, dynamic characteristics of the seismic loading and temporal variations in material properties. The seismic analyses accounted for both gravity and internal pressure loads. The findings of these analyses are detailed in the subsequent sections.

4.2.1. Modal spectral analysis

The structural responses of a lunar habitat due to shallow moonquakes with varying intensities are analyzed using the DMSA. Four load cases corresponding to T_r of 75, 475, 970 and 2475 years are considered and the stress distributions are obtained as shown in Fig. 12 (a) to (d). As anticipated, the tensile stresses are not uniformly distributed along the structure's walls, with the maximum values occurring at the connection between the main structure and the support. The σ_t and its respective percentage of σ_{tu} for each seismic case are summarized in Table 3. The stresses shown in Table 3 from the linear spectral analysis are compared with the material's maximum tensile stress. The results indicate that none of the four cases produced tensile stresses exceeding σ_{tu}. However, it is evident from the DMSA findings that shallow moonquakes with T_r greater than 75 years could generate stresses exceeding $0.5\sigma_{tu}$. At this stress level, the concrete could undergo plastic deformation and experience a degradation of its mechanical properties over time. To further investigate this phenomenon, it is necessary to evaluate the temporal response of the structure using the NRHA method.

Table 3. Maximum tensile stresses obtained from DMSA with CMS of frequent, rare, very rare and extremely rare shallow moonquakes.

T_r (years)	σ_t (MPa)	% σ_{tu}
75	2.55	45.54
475	3.53	63.04
970	4.03	71.96
2475	4.97	88.75

4.2.2. Nonlinear response history seismic analysis

A comprehensive analysis comprising 28 simulations is conducted to examine the response of the lunar habitat under seven pairs (x and y components) of ground

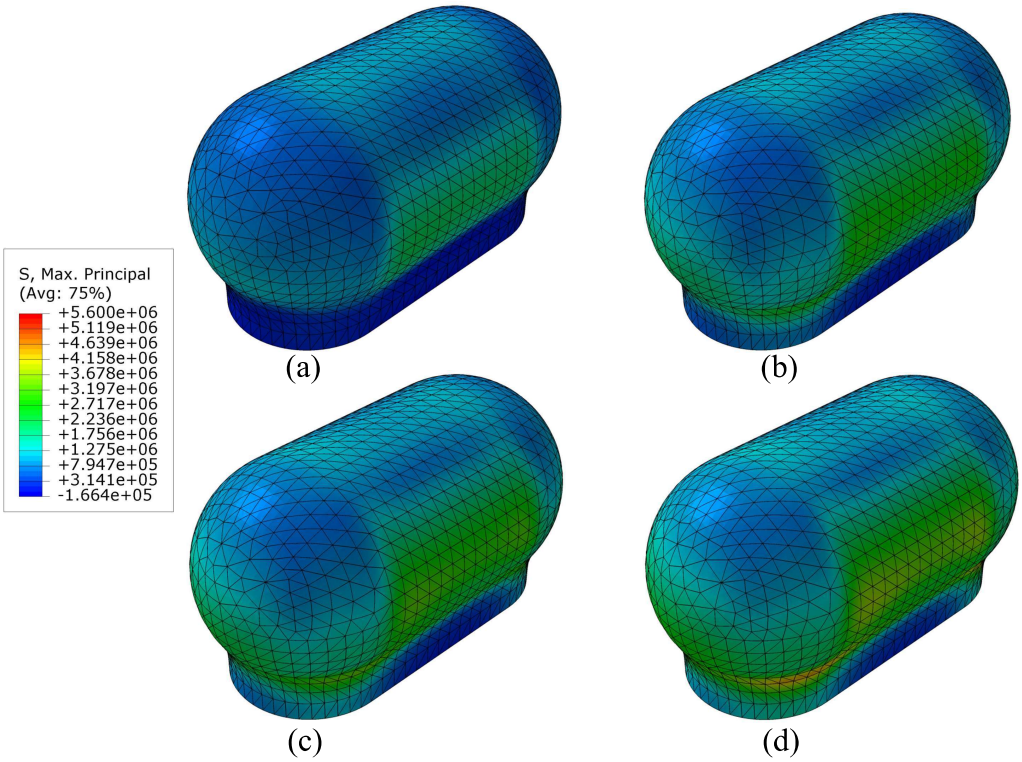

Fig. 12. Spatial distribution of tensile stresses generated by shallow moonquakes with a return period of: (a) 75, (b) 475, (c) 970 and (d) 2475 years, produced by DMSA.

motions. These ground motion pairs are scaled to four distinct intensity levels, with temporal and frequency characteristic adjustments to align with the study site's seismic hazard. The results of the simulations with GM scaled to represent shallow moonquakes with T_r of 75 years are presented in Table 4. Among the various connections within the structure, the interface between the main structure and the base exhibited the most significant plastic deformations in most cases. It is important to note that when the plastic strain exceeds 1.5×10^{-5} in the cylindrical structure, the structure's ability to withstand the stresses induced by internal pressure is compromised, resulting in structural failure. However, in the remaining cases where plastic deformation exceeded this threshold, the stability of the structure remains unaffected. The duration of the GMs significantly impacts the results of the temporal analyses due to the increasing deformations as the structure's stiffness degraded over time, especially during periods of high seismic displacements. A typical distribution of plastic deformations, depicted in Fig. 13, illustrates the

maximum deformation occurring at the connection between the base and the main structure, with regions exhibiting tensile plastic strains exceeding 1.5×10^{-5} are highlighted in red.

Table 4. Maximum plastic strains ϵ_{pmax} in the cylindrical structure (cs) and junction zone (jz) between the cylindrical structure and base generated by GM scaled to CMS of 75 years return period.

GM	ϵ_{pmax} in cs	ϵ_{pmax} in jz
1	1.30×10^{-5}	2.07×10^{-5}
2	1.10×10^{-5}	2.07×10^{-5}
3	1.19×10^{-5}	2.07×10^{-5}
4	1.50×10^{-5}*	3.08×10^{-5}
5	0	1.90×10^{-6}
6	1.35×10^{-5}	2.10×10^{-5}
7	7.61×10^{-7}	0

* In this simulation, the model experiences a complete loss of its ability to withstand internal pressure, resulting in an explosive failure.

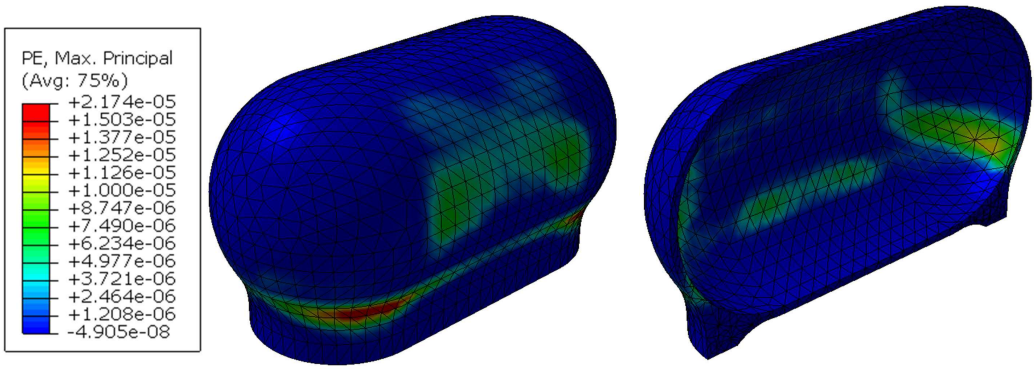

Fig. 13. Typical tensile plastic strains distribution generated by GM scaled to CMS of 75 years. (a) External view and (b) internal view.

The analysis of the lunar habitat under seven shallow moonquakes with T_r ranging from 475 to 2475 years reveals that the structural model experiences plastic deformations exceeding the material limit. When these deformations exceed a critical threshold, the structure loses its ability to withstand the loads induced by internal pressure, leading to catastrophic failure. The results from the NRHA

emphasize the significance of considering strength degradation when lunar habitats are exposed to ground motions with the intensity and duration characteristic of shallow moonquakes, even with shorter T_r. The prolonged seismic activity might progressively damage the structural materials, resulting in a complete loss of the structure's capacity to resist internal pressure loads. This phenomenon is not evident in the DMSA, emphasizing the importance of utilizing methods that directly capture the temporal behavior and account for all complexities that real structures may exhibit when designing seismic-resistant structures on the Moon.

This research addresses the significant seismic potential observed in various lunar regions, as highlighted in previous studies [12, 13, 82, 85]. Unique to this study is the utilization of seismograms that align with representative lunar seismic hazard spectra. In contrast with the work done by Mottaghi and Benaroya [24], our research incorporates a temporal seismic analysis that considers material non-linearity and the interaction between the structure and the regolith shield. By employing these advanced seismic analysis methods, this study provides a more realistic understanding of how a lunar habitat performs under seismic loads. Notably, these analysis techniques have also been recently applied to the seismic design of plain arches constructed from lunar materials [28]. The findings presented in this research emphasize the necessity of a detailed and comprehensive design approach to ensure the safety and resilience of lunar habitats subjected to seismic loads.

5. Conclusion

In this study, a seismic analysis of a lunar habitat constructed with lunar sulfur concrete is conducted. This study represents a pioneering effort in the seismic assessment of a long-term lunar habitat built with in situ resources using spectra generated specifically through probabilistic seismic hazard analysis of the Moon. Spectral- and time-domain methodologies were employed to analyze the seismic response of the lunar habitat. The spectral analysis provided an initial understanding of the habitat's behavior under seismic loading. However, the results of the temporal analysis revealed the importance of considering the degradation of mechanical properties over time when lunar habitats are subjected to extended seismic loading cycles. It was observed that a lunar habitat, which demonstrated satisfactory performance under gravity and internal pressure loading, might experience damage or even collapse when exposed to seismic loading. Hence, including seismic effects in the design of long-term lunar habitats is essential.

Based on the findings of this study regarding the structure's performance under seismic loading, it is recommended to incorporate lightweight and easily trans-

portable materials, such as Kevlar membranes, in conjunction with the structural concrete. This collaborative approach may effectively enhance the structure's ability to withstand the tensile stresses exerted by internal pressure. This study serves as a crucial first step towards implementing a performance-based design approach for lunar structures, laying the foundation for future research that will integrate updated seismic information obtained from ongoing and forthcoming seismic investigations on the Moon. With adequate seismic hazard studies and information on the necessary materials' mechanical properties, the methodology of this study can be applied to other extraterrestrial bodies, such as Mars. For future research, we recommend using a constitutive model obtained directly from experimental tests of sulfur concrete. Further studies should include the viscoelastic and aging behavior of the materials. It is worth mentioning that during the structure's lifetime, seismic loads and other types of hazards, such as meteorite impacts and radiation, may generate progressive deterioration in the structural materials of the proposed habitat. Hence, forthcoming research should assess the degradation of the structural material properties responsible for withstanding the loads generated by internal pressure. The decision-makers who will guide the planning and construction of future lunar bases should also consider this degradation of properties over time. Additionally, it is suggested that future investigations incorporate the site effects generated by soil layers on which the structure is located. Similarly, the seismic behavior of lunar structures subjected to moonquakes generated by meteorite impacts should be further evaluated in the future. Finally, it is suggested to complement the results of the numerical models with experimental setups of the full-scale structures.

6. Acknowledgments

The authors would like to acknowledge the financial support for the presented work provided by a research grant from the Universidad del Valle (Colombia), as part of the project "Performance-based design of a lunar habitat under seismic loading and meteorite impacts" (C.I. 21186). This work was supported in part by a Space Technology Research Institute Grant #80NSSC19K1076 from NASA's Space Technology Research Grants Program.

7. Declaration of competing interest

The authors declare that they have no known competing financial interests or personal relationships that could have appeared to influence the work reported in this paper.

References

[1] H. Benaroya, Lunar habitats: A brief overview of issues and concepts, Reach 7-8 (2017) 14–33. doi:10.1016/j.reach.2018.08.002.

[2] H. Benaroya, Building habitats on the moon: engineering approaches to lunar settlements, Springer, 2018.

[3] M. I. Allende, A. S. Kiremidjian, M. D. Lepech, D. J. Loftus, Performance-based engineering framework to quantify micrometeoroid damage to lunar surface structures, Journal of Aerospace Engineering 34 (5) (2021) 04021055. doi:10.1061/(ASCE)AS.1943-5525.0001300.

[4] M. Isachenkov, S. Chugunov, I. Akhatov, I. Shishkovsky, Regolith-based additive manufacturing for sustainable development of lunar infrastructure – an overview, Acta Astronautica 180 (2021) 650–678. doi:10.1016/j.actaastro.2021.01.005.

[5] NASA, Nasa's moon to mars strategy and objectives development (Apr 2023).
URL https://www.nasa.gov/sites/default/files/atoms/files/m2m_strategy_and_objectives_development.pdf

[6] A. K. Theinat, A. Modiriasari, A. Bobet, H. J. Melosh, S. J. Dyke, J. Ramirez, A. Maghareh, D. Gomez, Lunar lava tubes: Morphology to structural stability, Icarus 338 (2020) 113442. doi:10.1016/j.icarus.2019.113442.

[7] S. Dyke, A. Bobet, J. Ramirez, H. Melosh, D. Gomez, A. Maghareh, A. Modiriasari, A. Theinat, Resilient extraterrestrial habitat engineering, in: Lunar and Planetary Science Conference, Vol. 49, 2018, pp. 9–13.

[8] A. Maghareh, D. Gomez, S. Dyke, A. Bobet, J. Ramirez, H. Melosh, A. Modiriasari, A. Theinat, Resilience for permanent extraterrestrial habitats, in: Proceedings of the 48th Lunar and Planetary Science Conf, 2018, pp. 19–23.

[9] C. Nunn, R. Garcia, Y. Nakamura, A. Marusiak, T. Kawamura, D. Sun, L. Margerin, R. Weber, M. Drilleau, M. Wieczorek, A. Khan, A. Rivoldini, P. Lognonné, P. Zhu, Lunar seismology: A data and instrumentation review, Space Science Reviews 216 (5). doi:10.1007/s11214-020-00709-3.

[10] Y. Nakamura, Hft events: Shallow moonquakes?., Physics of the Earth and Planetary Interiors 14 (1977) 197–205.

[11] J. Oberst, Unusually high stress drops associated with shallow moonquakes, Journal of Geophysical Research: Solid Earth 92 (B2) (1987) 1397–1405. doi:10.1029/JB092iB02p01397.

[12] J. Oberst, Y. Nakamura, A seismic risk for the lunar base, in: 2nd Conference On Lunar Bases and Space Activities, Vol. 10, 1992, pp. 1397–1405.

[13] S. Ruiz, A. Cruz, D. Gomez, S. J. Dyke, J. Ramirez, Preliminary approach to assess the seismic hazard on a lunar site, Icarus 383 (2022) 115056. doi:10.1016/j.icarus.2022.115056.

[14] M. Banks, T. Watters, R. Weber, L. S. Schleicher, M. Bensi, N. Schmerr, Constructing a probabilistic seismic hazard analysis framework for the moon, 43rd COSPAR Scientific Assembly. Held 28 January-4 February 43 (2021) 358.

[15] J. W. Baker, Conditional mean spectrum: Tool for ground-motion selection, Journal of Structural Engineering 137 (3) (2011) 322–331. doi:10.1061/(ASCE)ST.1943-541X.0000215.

[16] B. Carlton, N. Abrahamson, Issues and Approaches for Implementing Conditional Mean Spectra in Practice, Bulletin of the Seismological Society of America 104 (1) (2014) 503–512. doi:10.1785/0120130129.

[17] N. Kalapodis, G. Kampas, O.-J. Ktenidou, A review towards the design of extraterrestrial structures: From regolith to human outposts, Acta Astronautica 175 (2020) 540–569. doi:10.1016/j.actaastro.2020.05.038.

[18] S. Ulubeyli, Lunar shelter construction issues: The state-of-the-art towards 3d printing technologies, Acta Astronautica 195 (2022) 318–343. doi:10.1016/j.actaastro.2022.03.033.

[19] R. B. Malla, D. Chaudhuri, Analysis of a 3d frame membrane structure for lunar base, in: Earth and Space, 2006, pp. 1–8. doi:10.1061/40830(188)61.

[20] H. Benaroya, Structures for manned habitation, in: Earth and Space, 2006, pp. 1–8. doi:10.1061/40830(188)78.

[21] R. B. Malla, T. G. Gionet, Dynamic response of a pressurized frame-membrane lunar structure with regolith cover subjected to impact load, Journal of Aerospace Engineering 26 (4) (2013) 855–873. doi:10.1061/(ASCE)AS.1943-5525.0000187.

[22] C. Zhou, B. Tang, L. Ding, P. Sekula, Y. Zhou, Z. Zhang, Design and automated assembly of planetary lego brick for lunar in-situ construction, Automation in Construction 118 (2020) 103282. doi:10.1016/j.autcon.2020.103282.

[23] L. C. Simonsen, M. J. Debarro, J. T. Farmer, Conceptual design of a lunar base thermal control system, in: 2nd Conference on Lunar Bases and Space Activities, 1992, pp. 579 – 591.

[24] S. Mottaghi, H. Benaroya, Design of a lunar surface structure. i: Design configuration and thermal analysis, Journal of Aerospace Engineering 28 (1) (2015) 04014052. doi:10.1061/(ASCE)AS.1943-5525.0000382.

[25] R. B. Malla, K. M. Brown, Determination of temperature variation on lunar surface and subsurface for habitat analysis and design, Acta Astronautica 107 (2015) 196–207. doi:10.1016/j.actaastro.2014.10.038.

[26] S. Tripathi, J. T. Steiner, R. B. Malla, Three-dimensional temperature profile in a dome-shaped habitat structure on the moon, Acta Astronautica 204 (2023) 263–280. doi:10.1016/j.actaastro.2022.12.040.

[27] S. Mottaghi, H. Benaroya, Design of a lunar surface structure. ii: Seismic structural analysis, Journal of Aerospace Engineering 28 (1) (2015) 04014053. doi:10.1061/(ASCE)AS.1943-5525.0000396.

[28] N. Kalapodis, G. Zalachoris, O.-J. Ktenidou, G. Kampas, On the seismic behaviour of monolithic lunar arches subjected to moonquakes, Earthquake Engineering & Structural Dynamics 52 (1) (2023) 147–163. doi:10.1002/eqe.3754.

[29] F. Ruess, J. Schaenzlin, H. Benaroya, Structural design of a lunar habitat, Journal of Aerospace Engineering 19 (3) (2006) 133–157. doi:10.1061/(ASCE)0893-1321(2006)19:3(133).

[30] P. S. Nowak, J. Janakus, C. E. Mitchell, Atmospheric pressure within lunar structure, Journal of Aerospace Engineering 7 (4) (1994) 398–410. doi:10.1061/(ASCE)0893-1321(1994)7:4(398).

[31] P. Francescato, A. Gillet, D. Leh, P. Saffré, Comparison of optimal design methods for type 3 high-pressure storage tanks, Composite Structures 94 (6) (2012) 2087–2096.

[32] P. M. Sforza, Commercial airplane design principles, Elsevier, 2014.

[33] K. J. Kennedy, A horizontal inflatable habitat for SEI, Space 92 (1992) 135–146.

[34] R. Dronadula, H. Benaroya, Hybrid lunar inflatable structure, Acta Astronautica 179 (2021) 42–55. doi:10.1016/j.actaastro.2020.10.039.

[35] J. Miller, L. Taylor, C. Zeitlin, L. Heilbronn, S. Guetersloh, M. DiGiuseppe, Y. Iwata, T. Murakami, Lunar soil as shielding against space radiation, Radiation Measurements 44 (2) (2009) 163–167. doi:10.1016/j.radmeas.2009.01.010.

[36] M. Roberts, Inflatable habitation for the lunar base, in: The Second Conference on Lunar Bases and Space Activities of the 21st Century, Volume 1, 1992, pp. 249 – 253.

[37] M. Arnhof, Design of a human settlement on mars using in-situ resources, in: 46th International Conference on Environmental Systems, 2016, pp. 1 – 15.

[38] F. Leckie, D. Bello, Strength and Stiffness of Engineering Systems, Mechanical Engineering Series, Springer US, 2010.

[39] M. Naser, Extraterrestrial construction materials, Progress in Materials Science 105 (2019) 100577. doi:10.1016/j.pmatsci.2019.100577.

[40] H. A. Toutanji, S. Evans, R. N. Grugel, Performance of lunar sulfur concrete in lunar environments, Construction and Building Materials 29 (2012) 444–448. doi:10.1016/j.conbuildmat.2011.10.041.

[41] A. M. Jablonski, K. A. Ogden, Technical requirements for lunar structures, Journal of Aerospace Engineering 21 (2) (2008) 72–90. doi:10.1061/(ASCE)0893-1321(2008)21:2(72).

[42] B. P. Kokelaar, R. S. Bahia, K. H. Joy, S. Viroulet, J. M. N. T. Gray, Granular avalanches on the moon: Mass-wasting conditions, processes, and features, Journal of Geophysical Research: Planets 122 (9) (2017) 1893–1925. doi:10.1002/2017JE005320.

[43] B. M. Das, N. Sivakugan, Fundamentals of geotechnical engineering, Cengage Learning, 2016.

[44] J. Wilson, F. Cucinotta, J. Miller, J. Shinn, S. Thibeault, R. Singleterry, L. Simonsen, M. Kim, Materials for shielding astronauts from the hazards of space radiations, MRS Online Proceedings Library (OPL) 551 (1998) 3.

[45] V. Aulesa, Architecture of lunar habitats, in: Exploration and Utilisation of the Moon, Vol. 462, 2000, p. 289.

[46] A. Goulas, R. J. Friel, 3D printing with moondust, Rapid Prototyping Journal 22 (2016) 864–870. doi:10.1108/RPJ-02-2015-0022.

[47] G. Bevan, G. Heiken, D. Vaniman, B. French, J. Schmitt, Lunar, P. Institute, Lunar Sourcebook: A User's Guide to the Moon, Cambridge University Press, 1991.

[48] B. Khoshnevis, J. Zhang, Extraterrestrial construction using contour crafting, in: 2012 International Solid Freeform Fabrication Symposium, University of Texas at Austin, 2012, pp. 250–259.

[49] G. Cesaretti, E. Dini, X. De Kestelier, V. Colla, L. Pambaguian, Building components for an outpost on the Lunar soil by means of a novel 3D printing technology, Acta Astronautica 93 (2014) 430–450. doi:10.1016/j.actaastro.2013.07.034.

[50] H. Toutanji, B. Glenn-Loper, B. Schrayshuen, Strength and durability performance of waterless lunar concrete, in: 43rd AIAA Aerospace Sciences Meeting and Exhibit, 2005, p. 1436.

[51] C. Meyers, H. Toutanji, Analysis of lunar-habitat structure using waterless concrete and tension glass fibers, Journal of Aerospace Engineering 20 (4) (2007) 220–226. doi:10.1061/(ASCE)0893-1321(2007)20:4(220).

[52] M. H. Shahsavari, M. M. Karbala, S. Iranfar, V. Vandeginste, Martian and lunar sulfur concrete mechanical and chemical properties considering

regolith ingredients and sublimation, Construction and Building Materials 350 (2022) 128914. doi:10.1016/j.conbuildmat.2022.128914.

[53] R. N. Grugel, H. Toutanji, Sulfur "concrete" for lunar applications–sublimation concerns, Advances in Space Research 41 (1) (2008) 103–112.

[54] R. Grugel, Sulfur'concrete'for lunar applications-environmental considerations, Tech. rep. (2008).

[55] D. Tucker, E. Ethridge, H. Toutanji, Production of glass fibers for reinforcement of lunar concrete, in: 44th AIAA aerospace sciences meeting and exhibit, 2006, p. 523.

[56] H. Toutanji, R. N. Grugel, Mechanical properties and durability performance of" waterless concrete", in: Earth & Space 2008: Engineering, Science, Construction, and Operations in Challenging Environments, 2008, pp. 1–8.

[57] W. N. Houston, J. K. Mitchell, I. Carrier, W. D., Lunar soil density and porosity, Lunar and Planetary Science Conference Proceedings 3 (1974) 2361–2364.

[58] M. M. Vlahovic, S. P. Martinovic, T. D. Boljanac, P. B. Jovanic, T. D. Volkov-Husovic, Durability of sulfur concrete in various aggressive environments, Construction and Building Materials 25 (10) (2011) 3926–3934. doi:10.1016/j.conbuildmat.2011.04.024.

[59] J. E. Colwell, S. Batiste, M. Horányi, S. Robertson, S. Sture, Lunar surface: Dust dynamics and regolith mechanics, Reviews of Geophysics 45 (2). doi:10.1029/2005RG000184.

[60] C. He, Geotechnical characterization of lunar regolith simulants, Ph.D. thesis, Case Western Reserve University (2010).

[61] R. Fediuk, M. Amran, M. Mosaberpanah, A. Danish, M. El-Zeadani, S. Klyuev, N. Vatin, A critical review on the properties and applications of sulfur-based concrete, Materials 13 (2020) 4712. doi:10.3390/ma13214712.

[62] Eurocode, Eurocode 2: Design of concrete structures, Part 1 1 (2004) 230.

[63] S. Brzev, J. Pao, Reinforced Concrete Design–a Practical Approach, Pearson Education Canada, 2006.

[64] S. Carmona, A. Aguado, New model for the indirect determination of the tensile stress–strain curve of concrete by means of the brazilian test, Materials and structures 45 (10) (2012) 1473–1485. doi:10.1617/s11527-012-9851-0.

[65] R. Evans, M. Marathe, Microcracking and stress-strain curves for concrete in tension, Matériaux et Construction 1 (1968) 61–64.

[66] R. L. Clough, K. T. Gillen, Combined environment aging effects: Radiation-thermal degradation of polyvinylchloride and polyethylene, Journal of Polymer Science: Polymer Chemistry Edition 19 (8) (1981) 2041–2051.

[67] R. B. Malla, A. Ghoshal, On thermally-induced vibrations of structures in space, Progress in Astronautics and Aeronautics 168 (1995) 68–95.

[68] N. Caluk, A. Azizinamini, Introduction to the concept of modular blocks for lunar infrastructure, Acta Astronautica 207 (2023) 153–166. doi:10.1016/j.actaastro.2023.03.004.

[69] K. Rojdev, M. J. E. O'Rourke, C. Hill, S. Nutt, W. Atwell, Radiation effects on composites for long-duration lunar habitats, Journal of Composite Materials 48 (7) (2014) 861–878.

[70] E. P. Steinberg, W. Bulleit, Reliability analyses of meteoroid loading on lunar structures, Structural Safety 15 (1) (1994) 51–66, special Issue on Reliability on Special Structural Systems. doi:10.1016/0167-4730(94)90052-3.

[71] Abaqus, ABAQUS/Standard User's Manual, Version 6.9, Dassault Systèmes Simulia Corp, United States, 2009.

[72] H. Benaroya, L. Bernold, Engineering of lunar bases, Acta Astronautica 62 (4) (2008) 277–299. doi:10.1016/j.actaastro.2007.05.001.

[73] C. Nunn, Y. Nakamura, S. Kedar, M. P. Panning, A new archive of apollo's lunar seismic data, The Planetary Science Journal 3 (9) (2022) 219. doi:10.3847/PSJ/ac87af.

[74] R. Yamada, The description of apollo seismic experiments, Japan Aerospace Exploration Agency. https://darts. isas. jaxa. jp/planet/seismology/apollo/The_Description_of_Apollo_Seismic_Experiments. pdf.

[75] G. Latham, M. Ewing, J. Dorman, D. Lammlein, F. Press, N. Toksoz, G. Sutton, F. Duennebier, Y. Nakamura, Moonquakes, Science 174 (4010) (1971) 687–692. doi:10.1126/science.174.4010.687.

[76] Y. Nakamura, G. V. Latham, H. J. Dorman, Apollo lunar seismic experiment—final summary, Journal of Geophysical Research 87 (S01) (1982) A117. doi:10.1029/jb087is01p0a117.

[77] Y. Nakamura, Farside deep moonquakes and deep interior of the moon, Journal of Geophysical Research: Planets 110 (E1). doi:10.1029/2004JE002332.

[78] F. Duennebier, G. H. Sutton, Thermal moonquakes, Journal of Geophysical Research 79 (29) (1974) 4351–4363. doi:10.1029/JB079i029p04351.

[79] G. Latham, J. Dorman, F. Duennebier, M. Ewing, D. Lammlein, Y. Nakamura, Moonquakes, meteoroids, and the state of the lunar interior, in: Lunar and Planetary Science Conference Proceedings, Vol. 4, 1973, p. 2515.

[80] Y. Nakamura, G. V. Latham, H. J. Dorman, A.-B. Ibrahim, J. Koyama, P. Horvath, Shallow moonquakes-depth, distribution and implications as to the present state of the lunar interior, in: Lunar and Planetary Science Conference Proceedings, Vol. 10, 1979, pp. 2299–2309.

[81] N. R. Goins, A. M. Dainty, M. N. Toksöz, Seismic energy release of the moon, Journal of Geophysical Research: Solid Earth 86 (B1) (1981) 378–388. doi:10.1029/JB086iB01p00378.

[82] R. Mohanty, P. S. Kumar, S. T. G. Raghukanth, K. J. P. Lakshmi, The long-lived and recent seismicity at the lunar orientale basin: Evidence from morphology and formation ages of boulder avalanches, tectonics, and seismic ground motion, Journal of Geophysical Research: Planets 125 (12) (2020) 10–22. doi:10.1029/2020JE006553.

[83] T. R. Watters, R. C. Weber, G. C. Collins, I. J. Howley, N. C. Schmerr, C. L. Johnson, Shallow seismic activity and young thrust faults on

the Moon, Nature Geoscience 12 (6) (2019) 411–417. doi:10.1038/s41561-019-0362-2.

[84] S. Ceylan, J. F. Clinton, D. Giardini, S. C. Stähler, A. Horleston, T. Kawamura, M. Böse, C. Charalambous, N. L. Dahmen, M. van Driel, C. Durán, F. Euchner, A. Khan, D. Kim, M. Plasman, J.-R. Scholz, G. Zenhäusern, E. Beucler, R. F. Garcia, S. Kedar, M. Knapmeyer, P. Lognonné, M. P. Panning, C. Perrin, W. T. Pike, A. E. Stott, W. B. Banerdt, The marsquake catalogue from insight, sols 0–1011, Physics of the Earth and Planetary Interiors 333 (2022) 106943. doi:10.1016/j.pepi.2022.106943.

[85] A. Mishra, S. Kumar, Spatial and temporal distribution of lobate scarps in the lunar south polar region: Evidence for latitudinal variation of scarp geometry, kinematics and formation ages, neo-tectonic activity and sources of potential seismic risks at the artemis candidate landing regions, Geophysical Research Letters 49 (18) (2022) 1–15. doi:10.1029/2022GL098505.

[86] S. Zielinski, Nasa's plans for moon base, Eos, Transactions American Geophysical Union 87 (52) (2006) 594–594. doi:10.1029/2006EO520003.

[87] B. L. Sharpe, D. G. Schrunk, An operationally ideal location for the first permanent base on the moon, in: Seventh International Conference and Exposition on Engineering, Construction, Operations, and Business in Space, 2000, pp. 777–783. doi:10.1061/40479(204)93.

[88] K. Sanderson, Age makes moon crater attractive site for lunar base (2008). doi:10.1038/news.2008.987.

[89] T. Hughes, The Finite Element Method: Linear Static and Dynamic Finite Element Analysis, Dover Civil and Mechanical Engineering, Dover Publications, 2012.

[90] Y. Tsompanakis, Earthquake Return Period and Its Incorporation into Seismic Actions, Springer Berlin Heidelberg, Berlin, Heidelberg, 2015, pp. 818–851. doi:10.1007/978-3-642-35344-4_116.

[91] FEMA, Nehrp recommended seismic provisions for new buildings and other structures, volume 1: Part 1 provisions, part 2 commentary, fema p-1050-1 (2015).

[92] F. Ferreira, C. Moutinho, A. Cunha, E. Caetano, An artificial accelerogram generator code written in Matlab, Engineering Reports 2 (3) (2020) e12129. doi:10.1002/eng2.12129.

[93] J. Vemuri, S. Kolluru, Evaluation of ground motion scaling techniques, in: Advances in Computer Methods and Geomechanics: IACMAG Symposium 2019 Volume 1, Springer, 2020, pp. 525–535.

[94] E. Kalkan, N. Luco, Special issue on earthquake ground-motion selection and modification for nonlinear dynamic analysis of structures (2011).

[95] ASCE, Seismic Design Criteria for Structures, Systems, and Components in Nuclear Facilities, asce/sei 43-05 Edition, American Society of Civil Engineers, 2005. doi:10.1061/9780784407622.

[96] J. Lubliner, J. Oliver, S. Oller, E. Oñate, A plastic-damage model for concrete, International Journal of Solids and Structures 25 (3) (1989) 299–326. doi:10.1016/0020-7683(89)90050-4.

[97] J. Lee, G. L. Fenves, Plastic-damage model for cyclic loading of concrete structures, Journal of Engineering Mechanics 124 (8) (1998) 892–900. doi:10.1061/(ASCE)0733-9399(1998)124:8(892).

[98] J. Xiao, H. Liu, T. Ding, Finite element analysis on the anisotropic behavior of 3d printed concrete under compression and flexure, Additive Manufacturing 39 (2021) 101712. doi:10.1016/j.addma.2020.101712.

[99] J. Y. Wu, J. Li, R. Faria, An energy release rate-based plastic-damage model for concrete, International Journal of Solids and Structures 43 (3) (2006) 583–612. doi:10.1016/j.ijsolstr.2005.05.038.

[100] T. Jankowiak, T. Lodygowski, Identification of parameters of concrete damage plasticity constitutive model, Foundations of civil and environmental engineering 6 (1) (2005) 53–69.

[101] H. Behnam, J. Kuang, B. Samali, Parametric finite element analysis of rc wide beam-column connections, Computers Structures 205 (2018) 28–44. doi:10.1016/j.compstruc.2018.04.004.